

A new analytical model for the non-linear clustering of dark matter halos

Charles Jose^{1,2*}, Cedric G. Lacey³ and Carlton M. Baugh³

¹*SB College, Changanassery, Kottayam 686101, Kerala, India*

²*IUCAA, Post Bag 4, Pune University Campus, Ganeshkhind, Pune 411007, India*

³*Institute for Computational Cosmology, Department of Physics, University of Durham, South Road, Durham DH1 3LE*

23 April 2022

ABSTRACT

We investigate the spatial clustering of dark matter halos, collapsing from $1 - 4\sigma$ fluctuations, in the redshift range $0 - 5$ using N-body simulations. The halo bias of high redshift halos ($z \geq 2$) is found to be strongly non-linear and scale-dependent on quasi-linear scales that are larger than their virial radii ($0.5 - 10$ Mpc/h). However, at lower redshifts, the scale-dependence of non-linear bias is weaker and is of the order of a few percent on quasi-linear scales at $z \sim 0$. We find that the redshift evolution of the scale dependent bias of dark matter halos can be expressed as a function of four physical parameters: the peak height of halos, the non-linear matter correlation function at the scale of interest, an effective power law index of the *rms* linear density fluctuations and the matter density of the universe at the given redshift. This suggests that the scale-dependence of halo bias is not a universal function of the dark matter power spectrum, which is commonly assumed. We provide a fitting function for the scale dependent halo bias as a function of these four parameters. Our fit reproduces the simulation results to an accuracy of better than 4% over the redshift range $0 \leq z \leq 5$. We also extend our model by expressing the non-linear bias as a function of the linear matter correlation function. Our results can be applied to the clustering of halos at any redshift, including those hosting early generations of stars or galaxies before reionization.

Key words: cosmology: theory – cosmology: large-scale structure of universe – galaxies: statistics – galaxy: haloes

1 INTRODUCTION

The spatial distribution of luminous galaxies is a valuable resource for probing cosmology and the physics of galaxy formation. The clustering of the galaxy distribution is shaped by the clustering of the dark matter halos which host them. The clustering of dark matter halos can be quantified using the halo bias which describes how dark matter halos trace the dark matter (Kaiser 1984; Bardeen et al. 1986; Bond et al. 1991). Conventional models assume that the halo bias is related to the underlying dark matter density field in a non-linear and deterministic fashion (Fry & Gaztanaga 1993). Mo & White (1996) showed that, on large scales, the halo bias can be approximated as a scale independent function of the mass of the halos. In particular, they showed that the clustering of dark matter halos is proportional to that of the dark matter with the constant of proportionality being called the linear halo bias. The approximation for

the clustering of halos using scale independent, linear bias is expected to be valid on scales larger than the virial radii of halos where dark matter halo substructure is not important.

However, the simple picture of a scale-independent halo bias has been shown to be inaccurate and various non-linear and non-local processes result in some degree of scale dependence (Matsubara 1999; Cole et al. 2005; Seo & Eisenstein 2005; Angulo et al. 2005; Huff et al. 2007; Smith et al. 2007; Angulo et al. 2008; Desjacques et al. 2010; Musso et al. 2013; Paranjape et al. 2013). Incorporating such a scale dependence of halo bias into theoretical models could be crucial for interpreting the clustering of galaxies. While several studies have focussed on the scale dependence of the bias on very large scales, its scale dependence on scales larger than the typical virial radii of dark matter halos is equally interesting. These scales, corresponding to comoving length scales of 0.1 to a few megaparsecs, are smaller than scales where the matter distribution is still linear and therefore are referred to as quasi-linear scales. The scale-dependence of halo bias on these scales arises mainly due to the non-linear

* charlesmanimala@gmail.com

growth of matter fluctuations (Smith et al. 2007) and is difficult to estimate using perturbative approaches because of the non-linearity of matter density field (Reed et al. 2009).

There have been studies in the literature of deviations from the linear bias approximation on quasi-linear scales using analytic techniques (Scannapieco & Barkana 2002; Iliev et al. 2003; Scannapieco & Thacker 2005) as well as N-body simulations (Hamana et al. 2001; Diaferio et al. 2003; Cen et al. 2004; Tinker et al. 2005; Gao et al. 2005; Angulo et al. 2008; Reed et al. 2009). In particular, these studies focussed on the clustering of dark matter halos either in the local universe (eg. Tinker et al. 2005) or at very high redshifts before the reionization of the intergalactic medium (Reed et al. 2009). In general these studies showed that the halo bias is non-linear and scale-dependent on quasi-linear scales, but the scale dependence weakens on large scales. Specifically, Reed et al. (2009) find a strong scale dependence of halo bias on quasi-linear scales for rare dark matter halos at high redshift, with the scale dependence increasing with the rarity of the halo.

The motivation of this paper is to study the clustering of dark matter halos with a specific focus on the scale dependence of halo bias on quasi-linear scales. In particular, we will focus on the redshift range $0 - 5$ where, to our knowledge, no such previous studies have been carried out. This will help to gauge the amplitude, scale dependence and evolution of the bias of dark matter halos for $0 \leq z \leq 5$ and hence bridge the gap between other studies which focus on the epochs before reionization. We will address this issue using N-body simulations to measure the dark matter and halo correlation functions in the real space. These measurements will be used to calibrate the nature and evolution of the non-linear halo bias in the redshift range $0 - 5$ over a range of length scales. In particular, we find that the bias of dark matter halos is non-linear and scale dependent on quasi-linear scales. Furthermore, it is not possible to express this scale dependence in terms of the usual parameterizations and therefore one has to invoke additional parameters.

The organization of this paper is as follows. In Section 2, we compare the halo bias of rare high redshift dark matter halos computed from analytic models and simulations. In Section 3, using simulations, we probe the scale dependence and redshift evolution of the non-linear bias of rare halos in the redshift range 0 to 5 and obtain a fitting function to describe these effects. We conclude with a brief discussion of our results and their implications in the final section.

2 CLUSTERING OF RARE DARK MATTER HALOS AT HIGH-Z

In this section, we investigate whether the linear bias model for halo clustering gives a good description of the clustering of high- z dark matter halos on quasi-linear scales. For this we first describe the linear bias model for halo clustering in Section 2.1. In Section 2.2 we introduce the N-body simulations used in our study. The clustering of dark matter halos estimated from these simulations is then compared with the clustering prediction using the linear bias model.

2.1 The linear bias model for halo clustering

In the linear bias approximation, the cross-correlation between halos of mass M' and M'' is given by

$$\xi_{hh}(r|M', M'', z) = b(M', z)b(M'', z)\xi_{mm}(r, z), \quad (1)$$

where $\xi_{mm}(r, z)$ is the non-linear two point correlation function of matter density contrast at redshift z and $b(M, z)$ is the scale independent linear bias of halos of mass M at this redshift. Eq. (1) is valid on large scales, where density perturbations grow linearly with redshift (Cooray & Sheth 2002). The two-point matter correlation function is obtained by Fourier transforming the non-linear matter power spectrum, $P(k, z)$ (Smith et al. 2003)

$$\xi_{mm}(r, z) = \int_0^\infty \frac{dk}{2\pi^2} k^2 P(k, z) \frac{\sin(kr)}{kr}. \quad (2)$$

It is well known that the scale independent halo bias can be expressed as a function of the ‘peak height’, $\nu(M, z) = \delta_c/\sigma(M, z)$, of dark matter halos (Mo & White 1996; Sheth & Tormen 1999; Sheth et al. 2001; Cooray & Sheth 2002; Tinker et al. 2010). The peak height is a measure of the rarity of halos (Sheth et al. 2001) with rarer halos having larger $\nu(M, z)$. Here, $\delta_c = 1.686$ is the critical density for halo collapse and $\sigma(M, z)$ is the *rms* linear density fluctuation on a mass scale M

$$\sigma^2(M, z) = \sigma^2(R, z) = \int_0^\infty \frac{dk}{2\pi^2} k^2 P^{lin}(k, z) W^2(k, R), \quad (3)$$

where R is the comoving radius of a sphere containing mass M , $W(k, R)$ is the Fourier transformation of the top hat window function and $P^{lin}(k, z)$ is the linear matter power spectrum.

In particular, for linear halo bias, we use the fitting function of Tinker et al. (2010) which was calibrated against N-body simulations and is given by,

$$b(M, z) = b(\nu(M, z)) = 1 - A \frac{\nu^a}{\nu^a + \delta_c^a} + B\nu^b + C\nu^c. \quad (4)$$

Tinker et al. (2010) estimate the free parameters of Eq. 4 to be $A = 1.0, a = 0.132, B = 0.183, b = 1.5, C = 0.265$ and $c = 2.4$. The halo bias given by Eq. (4) increases with increasing $\nu(M, z)$.

We assume that dark matter halos which can host galaxies have a spherical over-density $\Delta = 200$ times the average density of universe¹. Then, the virial radius r_{200} of a halo of mass M is $M = (4/3)\pi r_{200}^3 \rho_c \Delta$. Under the above assumptions the halo correlation function is

$$1 + \xi_{hh}(r|M', M'', z) = [1 + b(M', z)b(M'', z)\xi_{mm}(r)] \Theta[r - r_{\min}(M', M'')], \quad (5)$$

where the function $\Theta[r - r_{\min}(M', M'')]$ incorporates halo exclusion to ensure that $\xi_{hh}(r|M', M'', z) = -1$ for $r_{\min} = \max[r_{200}(M'), r_{200}(M'')]$.

¹ Tinker et al. (2010) calibrate their fitting function for the large scale bias as a function of Δ . Here, the quoted parameter values are for halos with $\Delta = 200$.

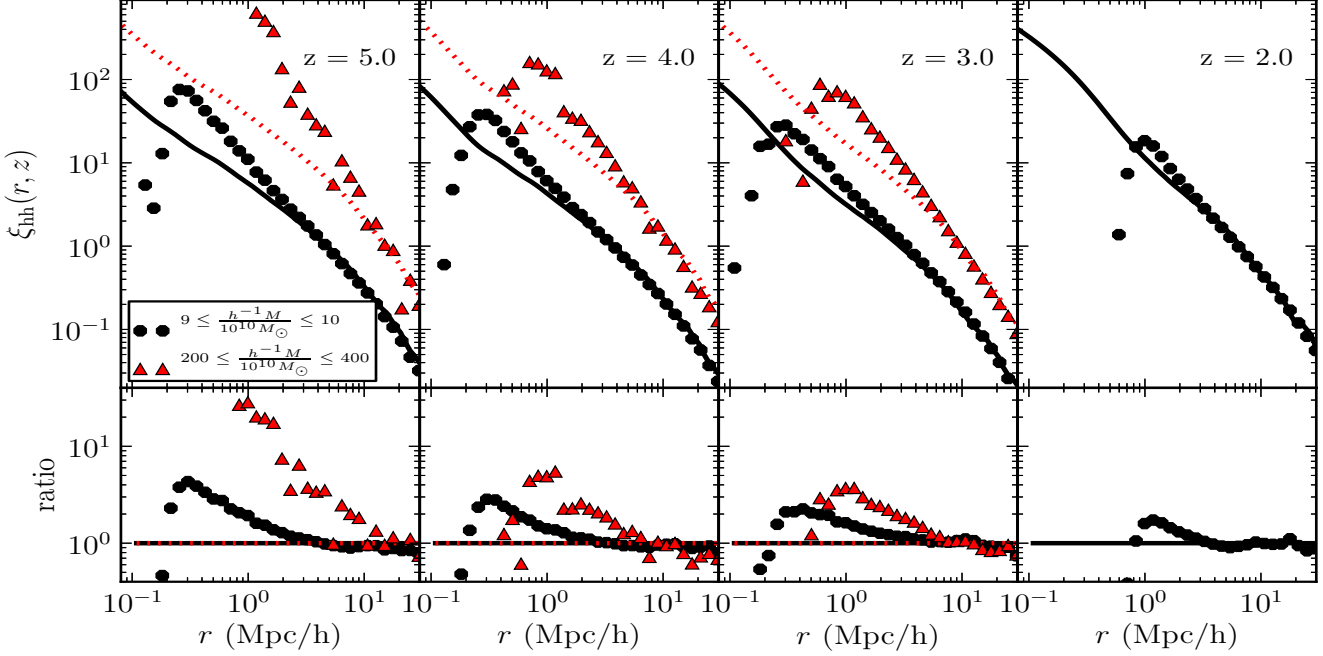


Figure 1. Upper panels : The two point correlation functions of dark matter halos in the mass range $\sim 10^{11} - 5 \times 10^{12} M_{\odot}$ at various redshifts as labelled. The points (triangles and circles) are measured from N-body simulations and the curves (solid and dotted) are analytic predictions using the linear bias approximation with the same cosmological parameters as used in the simulations. The results at $z = 2$ are from the MXXL simulation and those at other redshifts are from the MS-W7 simulation. Bottom panels: the ratio of the correlation functions measured from simulations to those computed analytically.

The two point correlation function of dark matter halos in a mass bin $M' \leq M \leq M''$ is given by

$$1 + \xi_{hh}(r|[M', M''], z) = \frac{1}{n^2([M', M''], z)} \int_{M'}^{M''} dM_1 \int_{M'}^{M''} dM_2 n(M_1) n(M_2) [1 + \xi_{hh}(r|M_1, M_2, z)], \quad (6)$$

where $n([M', M''], z) = \int_{M'}^{M''} dM n(M, z)$ is the total number density of halos in the mass bin $[M', M'']$. For the halo mass function, $n(M, z)$, we use the fitting function of Jenkins et al. (2001) which is in excellent agreement with the mass functions obtained from the simulations used in our study. Eq. (6) is a reasonable approximation for the usual 2-halo term for halo clustering on scales larger than the virial radii of dark matter halos (Cooray & Sheth 2002).

The average bias of halos with mass between M' and M'' , on scales bigger than their virial radii can be written as being scale-independent and is given by

$$b([M', M''], z) = \frac{1}{n([M', M''], z)} \int_{M'}^{M''} dM b(M, z) n(M, z). \quad (7)$$

Using this result for the bias in Eq. (6), we get

$$\xi_{hh}(r|[M', M''], z) = b^2([M', M''], z) \xi_{mm}(r, z). \quad (8)$$

In what follows, we will compute the halo correlation functions for dark matter halos in mass bins and compare with those measured from N-body simulations.

2.2 N-body simulations

Our study mainly uses two cosmological dark matter N-body simulations, the MS-W7 simulation (Guo et al. 2013; Pike et al. 2014) and the Millennium-XXL or MXXL simulation (Angulo et al. 2012). The MS-W7 simulation uses a cubic computational box of comoving length $500 h^{-1}$ Mpc with 2160^3 particles of mass $8.61 \times 10^8 M_{\odot}$. This is used to probe the clustering of halos at $z = 3, 4$ and 5 . It adopts a flat Λ CDM background cosmology, which is in agreement with the WMAP7 results (Larson et al. 2011), with $h = 0.704$, $\Omega_b = 0.0455$, $\Omega_c = 0.2265$, $\Omega_{\nu} = 0.0$, $\sigma_8 = 0.81$ and $n_s = 0.967$.

The MXXL extends the previous Millennium and Millennium-II simulations (Springel et al. 2005; Boylan-Kolchin et al. 2009) and follows the evolution of 6720^3 dark matter particles inside a cubic box of length $3000 h^{-1}$ Mpc. The particle mass is $8.46 \times 10^9 M_{\odot}$. This simulation adopts a Λ CDM cosmology with the same cosmological parameters as the previous Millennium simulations. Accordingly, $h = 0.73$, $\Omega_b = 0.045$, $\Omega_c = 0.205$, $\Omega_{\nu} = 0.0$, $\sigma_8 = 0.9$ and $n_s = 1.0$. The MXXL halos are used to investigate the clustering at $z = 0, 1, 2$ and 3 . We also compare the results obtained using MXXL simulation at $z = 3$ with those obtained using the Millennium simulation at the same redshift, which has a box of $500 h^{-1}$ Mpc.

In both simulations, groups of more than 20 particles are identified as dark matter halos using a friends-of-friends algorithm (FOF(0.2)) with linking parameter equal to 0.2 of the mean particle separation (Davis et al. 1985). The halo mass functions from these simulations are well described by

the fitting function of Jenkins et al. (2001) over a wide range of halo masses and to an accuracy better than 10 %.

The two point correlation functions of dark matter halos and dark matter particles from the simulations are computed by counting the number of pairs as a function of the separation, r , relative to that of a random distribution and is given by

$$\xi^{\text{sim}}(r) = \frac{N_p(r)}{N_{\text{ran}}^p(r)} - 1 \quad (9)$$

where $N_p(r)$ is the total number of pairs in the simulation separated by a distance r to $r + \delta r$ and $N_{\text{ran}}^p(r)$ is the total number of pairs.

As mentioned above, in this paper, we focus on the clustering of rare dark matter halos on quasi-linear scales in the redshift range 0 – 5. Therefore, we consider only those halos with a peak height $\nu(M, z) > 1$. At $z \sim 0$, the typical masses of these halos range between $10^{13} - 10^{15} M_\odot$ and therefore they correspond to poor galaxy groups and clusters. On the other hand, for $z \geq 2$, the masses of rare halos range from $10^{10} - 10^{13} M_\odot$. As we see later, the scale dependence of the halo bias due to non-linear clustering is much more significant at higher redshifts ($z = 2 - 5$) than it is at lower redshifts. Therefore, we first address the issue of the non-linear clustering of high redshift dark matter halos on quasi-linear scales and then its evolution in the low redshift universe.

2.3 Comparing simulations and linear bias models

We first demonstrate that the clustering strength of high- z , rare dark matter halos on quasi-linear scales differs significantly from the predictions of the linear bias model by comparing with the spatial correlation functions estimated from N-body simulations. In the top panels of Fig. 1, the halo correlation functions estimated from simulations ($\xi_{\text{hh}}^{\text{sim}}(M, r, z)$) are shown at $z = 2, 3, 4$ and 5 for halos in the mass range $9 \times 10^{10} - 10^{11} h^{-1} M_\odot$ (black circles) and $2 \times 10^{12} - 4 \times 10^{12} h^{-1} M_\odot$ (red triangles). We note that, these halos respectively host typical Lyman- α emitters (LAEs) and Lyman-break galaxies (LBGs) in the same redshift range (Jose et al. 2013b,a) and are rare halos, collapsing from $2 - 3\sigma$ fluctuations ($\nu(M, z) \sim 2 - 3$). On small scales the correlation functions drop to -1 due to halo exclusion. These scales correspond to the typical virial radius of halos in the given mass bin.

Also shown in the top panels of Fig. 1 are the correlation functions, $\xi_{\text{hh}}(M, r, z)$, predicted by the analytic model of Eq. (8) for the same cosmological parameters as used in the simulations. The correlation functions are computed for halos in the same mass bins used to estimate $\xi_{\text{hh}}^{\text{sim}}(M, r, z)$. Fig. 1 clearly shows that $\xi_{\text{hh}}^{\text{sim}}(r, z)$ and $\xi_{\text{hh}}(r, z)$ agree well with each other on large scales ($r \gtrsim 10 - 15 h^{-1}$ Mpc). However, on quasi-linear scales ($r \sim 0.5 - 10 h^{-1}$ Mpc), $\xi_{\text{hh}}^{\text{sim}}(r, z)$ determined from the simulations shows an excess compared to $\xi_{\text{hh}}(r, z)$ computed analytically.

To understand the degree of this deviation more clearly, we have plotted in the bottom panels of Fig. 1 the ratio of the dark matter halo correlation functions measured from simulations to that computed from the linear bias model (i.e. $\xi_{\text{hh}}^{\text{sim}}(r, z)/\xi_{\text{hh}}(r, z)$) for each mass bin. It is clear from

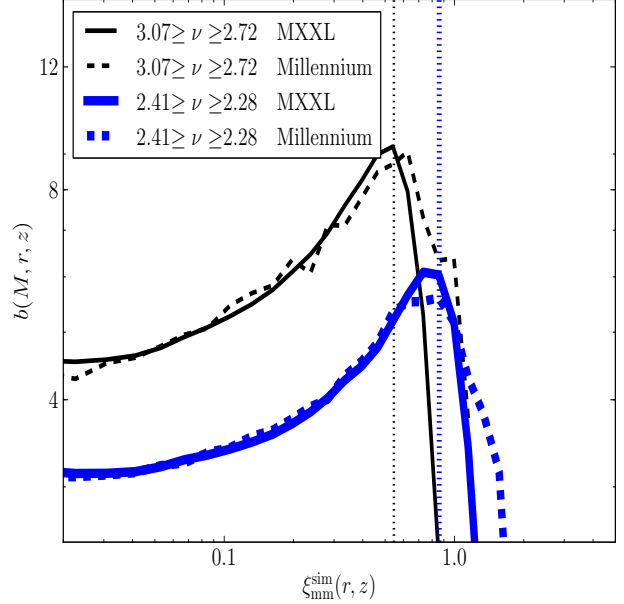


Figure 2. The halo bias $b(r, M, z) = \sqrt{\xi_{\text{hh}}^{\text{sim}}(r, z)/\xi_{\text{mm}}^{\text{sim}}(r, z)}$ computed at $z = 3$ using Millennium and MXXL halos in $\nu(M, z)$ bins, as indicated by the label. The thick (blue) and thin (black) lines respectively correspond to halos with $2.41 \geq \nu \geq 2.28$ and $3.07 \geq \nu \geq 2.72$. The thick (blue) and thin (black) vertical lines indicate scales corresponding to twice the virial radius of the most massive halo in each sample.

the figure that, on quasi-linear scales, the predictions of the scale-independent bias model are insufficient to explain the halo correlation functions measured directly from the simulations. For example, the massive halos at the highest redshift ($2 \times 10^{12} \leq M/M_\odot \leq 4 \times 10^{12}$ at $z = 5$) show clustering in the simulations that is sometimes larger by a factor as large as ~ 20 at $1 \leq r \leq 2$ Mpc/h, compared to the analytic predictions. On the other hand, at lower redshifts and for less massive halos ($9 \times 10^{10} \leq M/M_\odot \leq 10^{11}$ at $z = 3$), the clustering excess is only a factor of 2 – 3 at $r \sim 0.5$ Mpc/h. Furthermore, the deviation between $\xi_{\text{hh}}^{\text{sim}}(r, z)$ and $\xi_{\text{hh}}(r, z)$ increases with the redshift and mass of dark matter halos. Overall we conclude that the halo bias of high redshift dark matter halos is strongly scale dependent on quasi-linear scales and the scale dependence increases with the rarity of the halos.

Earlier studies focused on the non-linear bias of halos at the present epoch (Hamana et al. 2001; Diaferio et al. 2003; Tinker et al. 2005) or at redshifts before reionization (Reed et al. 2009). The scale dependence of the non-linear bias in the fitting functions provided by Hamana et al. (2001); Diaferio et al. (2003); Tinker et al. (2005) is too weak to explain the clustering of halos at the redshifts, masses and scales of interest here. The fitting function of Reed et al. (2009) has a stronger scale-dependence and describes the non-linear clustering of high redshift MS-W7 halos correctly. However, as we see later, their results are not consistent with the bias measured from the MXXL simulation and also at lower redshifts ($z = 0 - 2$). Therefore, non-linear clustering of rare halos on quasi-linear scales has not been satisfactorily addressed and thus warrants further investigation.

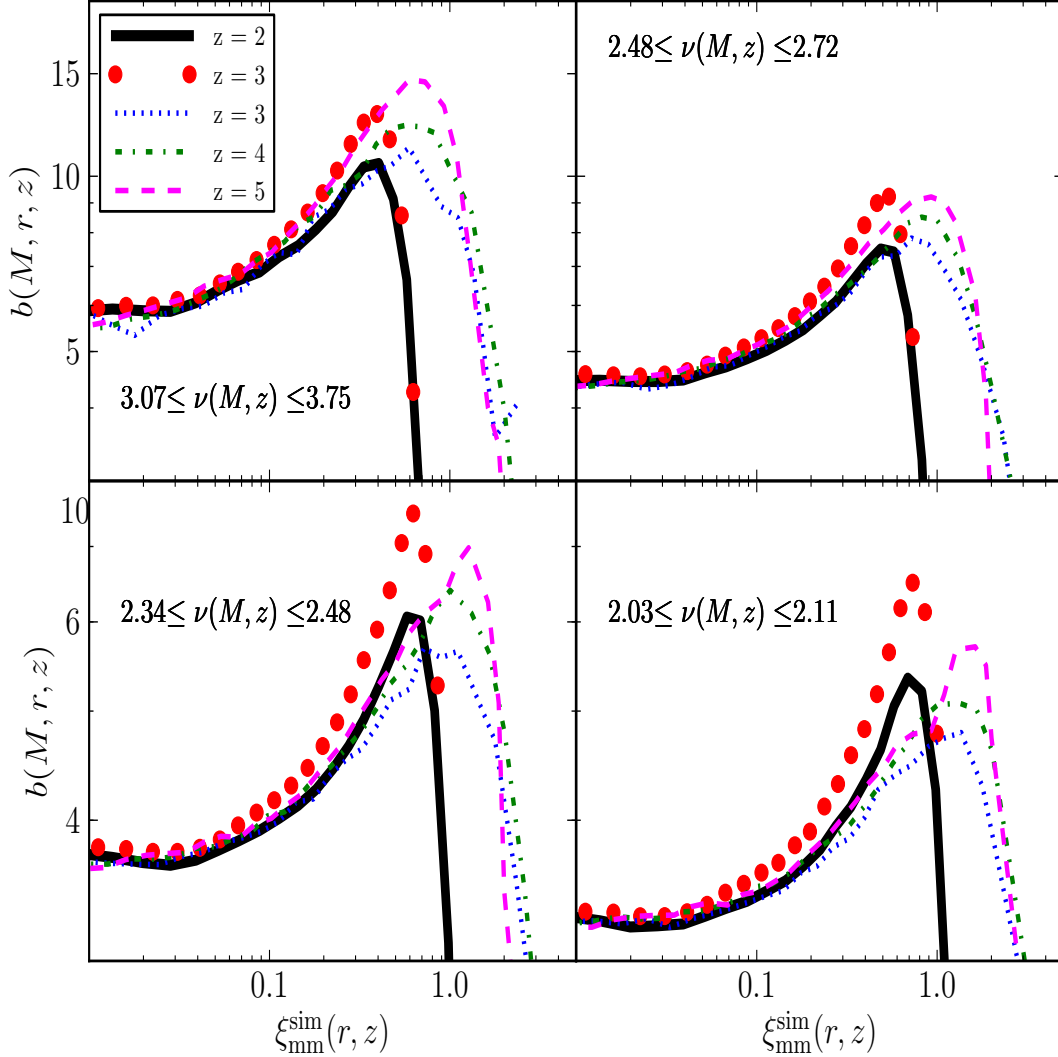


Figure 3. The halo bias $b(r, M, z) = \sqrt{\xi_{hh}^{\text{sim}}(r, z) / \xi_{mm}^{\text{sim}}(r, z)}$ plotted as a function of $\xi_{mm}^{\text{sim}}(r, z)$ in the redshift range 2 – 5. Each panel shows the $b(r, M, z)$ of halos in $\nu(M, z)$ bins, as indicated by the label. The results obtained from the MXXL simulation are shown by the solid black lines ($z = 2$) and red circles ($z = 3$) whereas other curves corresponds to the results from the MS-W7 simulation.

3 THE SCALE-DEPENDENT, NON-LINEAR HALO BIAS

3.1 The measured bias

We have shown in the previous section that, on quasi-linear scales, high- z dark matter halos collapsing from 2 – 3 σ fluctuations cluster more strongly than the predictions of the linear bias model. Therefore, to understand the clustering of these rare halos, one has to invoke a scale-dependent, non-linear bias. For this, we first define a non-linear, scale dependent halo bias of dark matter halos at any redshift as

$$b_{nl}(r, M, z) = \sqrt{\frac{\xi_{hh}^{\text{sim}}(r, z)}{\xi_{mm}^{\text{sim}}(r, z)}}. \quad (10)$$

Here, $\xi_{mm}^{\text{sim}}(r, z)$ is the non-linear dark matter correlation function computed directly from the simulations using Eq. (9). The function $b(r, M, z)$ is thus expected to be independent of r on large scales.

In the previous section, we estimated the clustering of halos in different mass bins. However, it would be more use-

ful if the non-linear bias could be calculated from the dark matter power spectrum. One could then hope to apply our results in more general contexts. Furthermore, as discussed in the previous section, we first focus on high redshift halos. Therefore, we measured the scale-dependent halo bias ($b_{nl}(r, M, z)$) of dark matter halos from the MS-W7, MXXL and Millennium simulations in bins of peak height, $\nu(M, z)$, in the redshift range 2 – 5.

First, we briefly discuss the effects of resolution and the halo exclusion effect on the estimated non-linear bias by comparing results obtained using MXXL and Millennium halos at $z = 3$. As discussed before, these simulations have the same set of cosmological parameters, but different mass resolutions and volumes. In Fig. 2, we have plotted the non-linear bias at $z = 3$ for halos (in a given ν bin) from the MXXL and Millennium simulations as a function of $\xi_{mm}^{\text{sim}}(r, z)$ at the same redshift. Also shown by the vertical line, is the length scale corresponding to twice the virial radius of the most massive halo in each sample.

It is clear from Fig. 2 that the halo bias estimated from

(ν_{\min}, ν_{\max}) ν_{av}	M_{av}/M_{\odot}								
	MXXL halos				MS-W7 halos			Millennium halos	
	$z=0$	$z=1$	$z=2$	$z=3$	$z=3$	$z=4$	$z=5$	$z=3$	
(3.37, 4.21) 3.77	1.9×10^{15}	3.0×10^{14}	6.1×10^{13}	1.5×10^{13}	8.0×10^{12}	2.7×10^{12}	7.4×10^{11}	1.5×10^{13}	
(3.07, 3.37) 3.22	1.2×10^{15}	1.8×10^{14}	3.3×10^{13}	7.7×10^{12}	3.9×10^{12}	1.2×10^{12}	3.1×10^{11}	7.7×10^{12}	
(2.81, 3.07) 2.93	8.9×10^{14}	1.2×10^{14}	2.1×10^{13}	4.5×10^{12}	2.2×10^{12}	6.5×10^{11}	1.6×10^{11}	4.5×10^{12}	
(2.59, 2.81) 2.70	6.5×10^{14}	8.2×10^{13}	1.3×10^{13}	2.7×10^{12}	1.3×10^{12}	3.6×10^{11}	8.0×10^{10}	2.7×10^{12}	
(2.44, 2.59) 2.52	5.0×10^{14}	5.9×10^{13}	9.2×10^{12}	1.8×10^{12}	8.0×10^{11}	2.1×10^{11}		1.8×10^{12}	
(2.28, 2.41) 2.34	3.7×10^{14}	4.2×10^{13}	6.0×10^{12}	1.1×10^{12}	4.8×10^{11}	1.2×10^{11}		1.1×10^{12}	
(2.19, 2.28) 2.23	3.0×10^{14}	3.3×10^{13}	4.6×10^{12}		3.4×10^{11}	8.2×10^{10}		8.0×10^{11}	
(2.11, 2.19) 2.15	2.6×10^{14}	2.7×10^{13}	3.6×10^{12}		2.5×10^{11}	5.9×10^{10}		6.1×10^{11}	
(2.03, 2.11) 2.07	2.2×10^{14}	2.2×10^{13}	2.9×10^{12}		1.9×10^{11}			4.7×10^{11}	
(1.96, 2.03) 2.00	1.9×10^{14}	1.8×10^{13}	2.3×10^{12}		1.4×10^{11}			3.6×10^{11}	
(1.87, 1.92) 1.89	1.5×10^{14}	1.4×10^{13}	1.6×10^{12}		9.2×10^{10}			2.5×10^{11}	
(1.77, 1.81) 1.79	1.2×10^{14}	1.0×10^{13}	1.1×10^{12}		5.8×10^{10}			1.6×10^{11}	
(1.69, 1.72) 1.70	9.2×10^{13}	7.5×10^{12}						1.1×10^{11}	
(1.53, 1.56) 1.55	5.8×10^{13}	4.2×10^{12}						4.9×10^{10}	
(1.30, 1.32) 1.31	2.5×10^{13}	1.5×10^{12}							
(1.12, 1.14) 1.13	1.1×10^{13}								

Table 1. Column 1: The $\nu(M, z)$ bins of halos used to calibrate the non-linear bias. Column 2: The corresponding average peak height, ν_{av} . Other columns give the average mass, M_{av} , of halos in the sample at the given redshift. If M_{av} is not given, then the $\nu(M, z)$ bin is not used in our analysis. Columns 3-6 results are for MXXL halos, columns 7-9 are for MS-W7 halos whereas column 10 refers to Millennium halos.

the two simulations agree well with one another on scales larger than twice the virial radius of the most massive halo in the sample. However, on smaller scales, the estimated halo bias is different between the two simulations. Since both simulations use the same set of cosmological parameters, this could be due to the difference in mass resolution between the simulations. We also note that, on the largest scales ($\xi_{\text{mm}}^{\text{sim}}(r, z) < 0.05$), the bias is approximately a constant. On smaller scales, the non-linear bias increases with decreasing scale (increasing $\xi_{\text{mm}}^{\text{sim}}$) and reaches a maximum value around the scale corresponding to twice the virial radius of the most massive halo in the sample. On smaller scales than this, the halo bias drops to 0. This suggest that, while probing the clustering of a sample of halos, the halo exclusion effect is important on scales smaller than twice the virial radius of the most massive halo in the sample. Because of these effects due to the resolution and halo exclusion, our further discussion and analysis will consider the clustering of a sample of halos only on scales larger than twice the virial radius of the most massive halo in that sample.

We now present our estimates of the non-linear bias from different simulations at various redshifts in Fig. 3 as a function of $\xi_{\text{mm}}^{\text{sim}}(r, z)$. The results measured from the MXXL simulation at $z = 2$ are shown by solid black lines and at $z = 3$ are shown using red circles. All the other curves at $z = 3, 4$ and 5 are estimates of $b_{nl}(r, M, z)$ from the MS-W7 simulation. Each panel corresponds to a different bin of $\nu(M, z)$ (see labels). We again emphasize that $b_{nl}(M, r, z)$

at a given redshift is plotted against $\xi_{\text{mm}}^{\text{sim}}(r, z)$ at the same redshift.

We first note that, on scales corresponding to $\xi_{\text{mm}}^{\text{sim}} \lesssim 0.1$, $b_{nl}(r, M, z)$ measured from the MS-W7 and MXXL simulations agree well with each other. On smaller scales, the estimated bias is different for the two simulations. The halo bias measured from the MXXL simulation drops to zero on larger scales compared to the bias estimated from the MS-W7 simulation. This is because, for halos in a given ν bin, the masses and virial radii of MXXL halos are larger than those of MS-W7 halos.

3.2 A model for the halo bias

As discussed before, $b_{nl}(r, M, z)$ at different redshifts is fairly constant for $\xi_{\text{mm}}^{\text{sim}} \lesssim 0.05$. These scales typically correspond to comoving length scales greater than $10 h^{-1}$ Mpc. Thus on such large scales, the expression for the non-linear bias reverts back to the usual scale-independent large scale bias, which is only a function of the peak height ν alone. Therefore, one can write

$$b_{nl}(r, M, z) = \gamma(r, M, z)b(\nu), \quad (11)$$

where $b(\nu)$ is the large scale bias. Here the non-linear bias, $b_{nl}(r, M, z)$, is written as the product of a scale-dependent function, $\gamma(r, M, z)$, and the large scale bias. The scale-dependent function $\gamma(r, M, z)$ is thus expected to be close to unity on large scales.

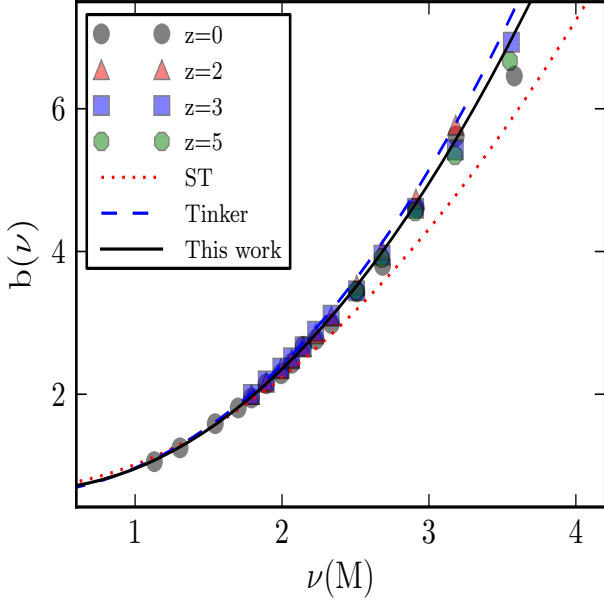


Figure 4. Our fit to Eq. (4) for the large scale linear halo bias (solid black curve) along with the simulation measurements (symbols) at various redshifts. The points for $z = 0$ and 2 are measured from the MXXL simulation and those at $z = 3$ and 5 are obtained from the MS-W7 simulation. The red dotted and blue dashed curves are the fitting functions of the linear halo bias given by Sheth & Tormen (1999) (ST) and Tinker et al. (2010) (Tinker) respectively.

To understand the evolution of the non-linear bias of rare halos with redshift, one has to calibrate the expressions for the large scale linear bias $b(\nu)$ and scale dependent function $\gamma(r, M, z)$. In what follows, we first obtain a fitting function for $b(\nu)$ and then constrain the functional form of $\gamma(r, M, z)$.

3.3 The large scale bias

To estimate $b(\nu)$, we measured the correlation functions of dark matter halos in different $\nu(M, z)$ bins in the redshift range $0 - 5$. These ν -bins are given in column 1 of Table 1. Also given in the table are the average peak height, ν_{av} and average mass of halos, M_{av} , in these bins at each redshift. The average peak height is given by $\nu_{av} = \delta_c / \sigma_{av}$, where σ_{av} is computed as

$$\sigma_{av}^2(z) = \frac{\int dM n(M, z) \sigma^2(M, z)}{\int dM n(M, z)}. \quad (12)$$

We define the large scale bias, $b(\nu)$, as the average bias of halos that are separated by $10 \leq r \leq 25$ Mpc/h, i.e.

$$b(\nu) = \sqrt{\frac{\int_{10}^{25} dr r^2 \xi_{hh}(\nu, \xi_{mm}^{sim}(r))}{\int_{10}^{25} dr r^2 \xi_{mm}^{sim}(r)}}. \quad (13)$$

We then obtain a fitting function for $b(\nu)$ by refitting the free parameters of Eq. (4) to the $b(\nu)$ measured from the simulations using Eq. (13). The best fit parameters are estimated to be $A = 1.0, a = 0.36, B = -1.156, b = 2.18, C = -0.749$ and $c = 2.18$, treating all bias values with equal weight. In Fig. 4, our fit (black solid line) for $b(\nu)$ is overplotted

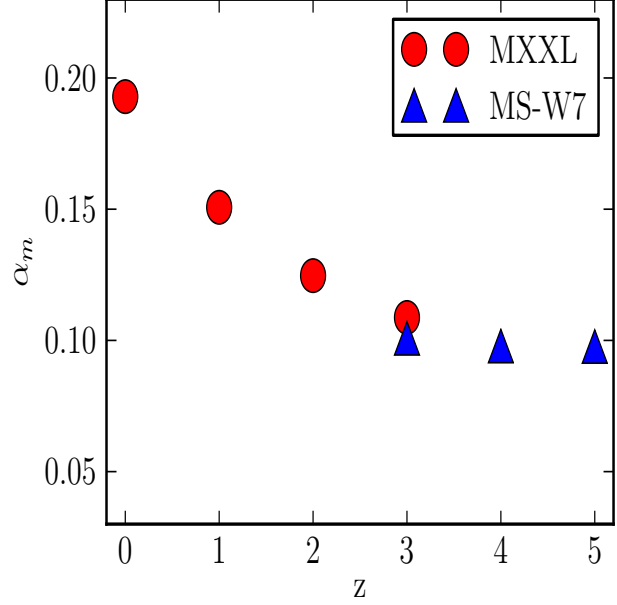


Figure 5. The effective power law index, α_m , (Eq. (14)) is plotted as a function of redshift. The blue triangles and red circles correspond to the values obtained for the MS-W7 and the MXXL cosmology respectively.

with the symbols measured directly from the simulation at different redshifts. The data points at $z = 0, 1$, and 2 are measured from the MXXL simulation and those at $z = 3, 4$, and 5 are obtained from MS-W7 simulation. It is clear from Fig. 4 that our fitting function for $b(\nu)$ agrees very well with the measurements from the simulations. In fact, we find that, the overall agreement between the simulation results and the analytic fit is within 3%. Also shown in Fig. 4 are the fitting functions for halo bias from Sheth & Tormen (1999) (ST, red dotted curve) and Tinker et al. (2010) (Tinker, blue dashed curve). One can see from the figure that when $\nu(M) \lesssim 2$, our formula compares well with these two fitting functions (particularly with the Tinker formula). However, for larger values of $\nu(M)$, the ST formula predicts lower bias values and Tinker formula gives slightly larger bias values compared with our formula for halo bias. Thus for rarer halos with $\nu \geq 2$, our analysis predicts a slightly lower value for the large scale bias compared to the Tinker formula. However, we also note that Tinker et al. (2010) use the spherical overdensity (SO) algorithm (Tinker et al. 2008) to identify halos, which is different from the FOF(0.2) algorithm used in this work. Such a difference in the bias of halos identified by these two algorithms has already been noted by Tinker et al. (2008, 2010). Further, the simulations used by Tinker et al. (2010) span a wider range of cosmological parameters than used in this work. This could also account for the difference between the estimated large scale halo bias.

3.4 The scale dependence of halo bias

Having obtained the expression for the large scale ($r \geq 10$ Mpc/h) bias of rare halos in the redshift range $0 - 5$, we now wish to calibrate the scale dependence $\gamma(M, r, z)$ of $b(r, M, z)$ on quasi-linear scales. We first concentrate on the expression for $\gamma(M, r, z)$ of halos in the redshift range $2 - 5$. This is

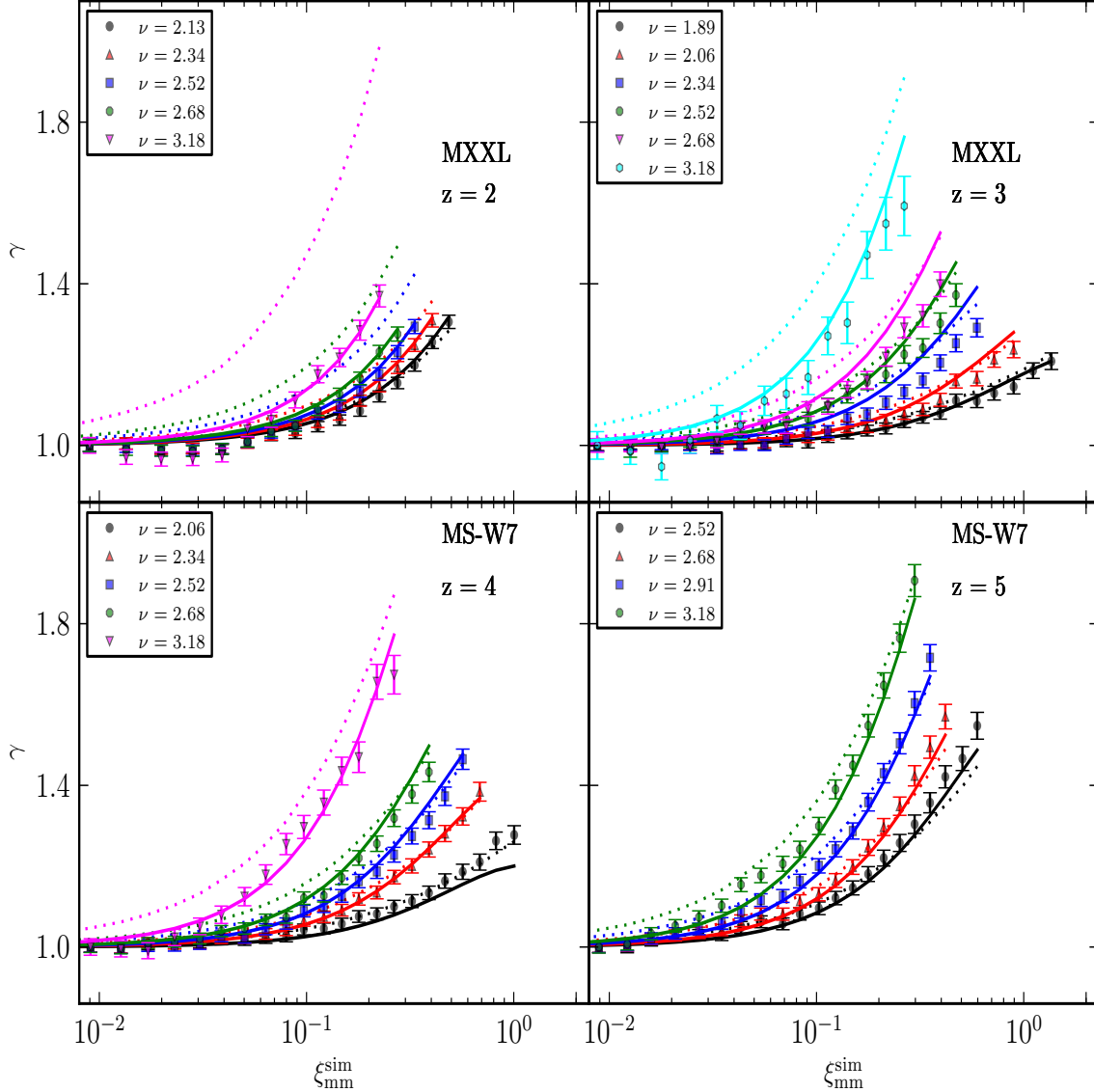


Figure 6. The scale dependence of non-linear bias, $\gamma(\xi_{\text{smm}}^{\text{sim}}, \nu, \alpha_m)$, measured from N-body simulations, in the redshift range $z = 2 - 5$ as a function of $\xi_{\text{smm}}^{\text{sim}}(r)$ for halos in the ν -bins listed in the legend. Solid lines: the fit for $\gamma(\xi_{\text{smm}}^{\text{sim}}, \nu, \alpha_m)$ presented in this work. Dotted lines: the fitting function for γ given by Reed et al. (2009).

because, as we shall see later, $\gamma(M, r, z)$ probably has an explicit dependence on the effective matter density $\Omega_m(z)$ of the universe as a function of redshift. We expect to separate out this dependence by focussing on high redshifts ($z \geq 2$) where $\Omega_m(z) \approx 1$.

It is clear from Fig. 3 that the scale dependent, non-linear bias of halos (from the MS-W7 simulation) of a given $\nu(M, z)$ as function of $\xi_{\text{smm}}^{\text{sim}}(r, z)$ and at $z = 3, 4$ and 5 , agree fairly well with each other. In fact, in this case, the agreement between estimates of $b(r, M, z)$ at different redshifts is better than 10 % on quasi-linear scales ($r \leq 15 h^{-1}$ Mpc). However, Fig. 3 shows that the scale dependence $b(r, M, z)$ of MXXL halos for the same $\nu(M, z)$ at $z = 2$ and 3 (which is also expressed as function of $\xi_{\text{smm}}^{\text{sim}}(r, z)$) is quite different from that of MS-W7 halos at higher redshift. Thus, $\gamma(M, r, z)$, which accounts for the scale dependence of $b(r, M, z)$, cannot be described as a function of just two variables, $\xi_{\text{smm}}^{\text{sim}}(r, z)$ and $\nu(M, z)$. This suggests that the non-

linear bias on quasi-linear scales is not a simple function of the dark matter power spectrum and any fitting function should have an explicit dependence on other parameters.

We find that adding one more parameter can account for all the simulation results in the redshift range $2 - 5$. That is, $\gamma(M, r, z)$ at $2 \leq z \leq 5$ can be expressed, to sufficient accuracy, as function of three variables, $\nu(M, z)$, $\xi_{\text{smm}}^{\text{sim}}(r, z)$ and $\alpha_m(z)$, an effective power law index of $\sigma(M, z)$. This effective power law index is defined as

$$\alpha_m(z) = \frac{\log(1.686)}{\log[M_{\text{nl}}(z)/M_{\text{col}}(z)]}, \quad (14)$$

where the non-linear mass scale, $M_{\text{nl}}(z)$, and the collapse mass scale, $M_{\text{col}}(z)$, at any redshift are masses at which the peak heights are, respectively, 1.686 and 1 (see Appendix A for more details). The dependence of $\gamma(M, r, z)$ on $\alpha_m(z)$ can be tentatively understood from Fig. 5, where we have plotted this ratio as a function of z . The blue triangles at

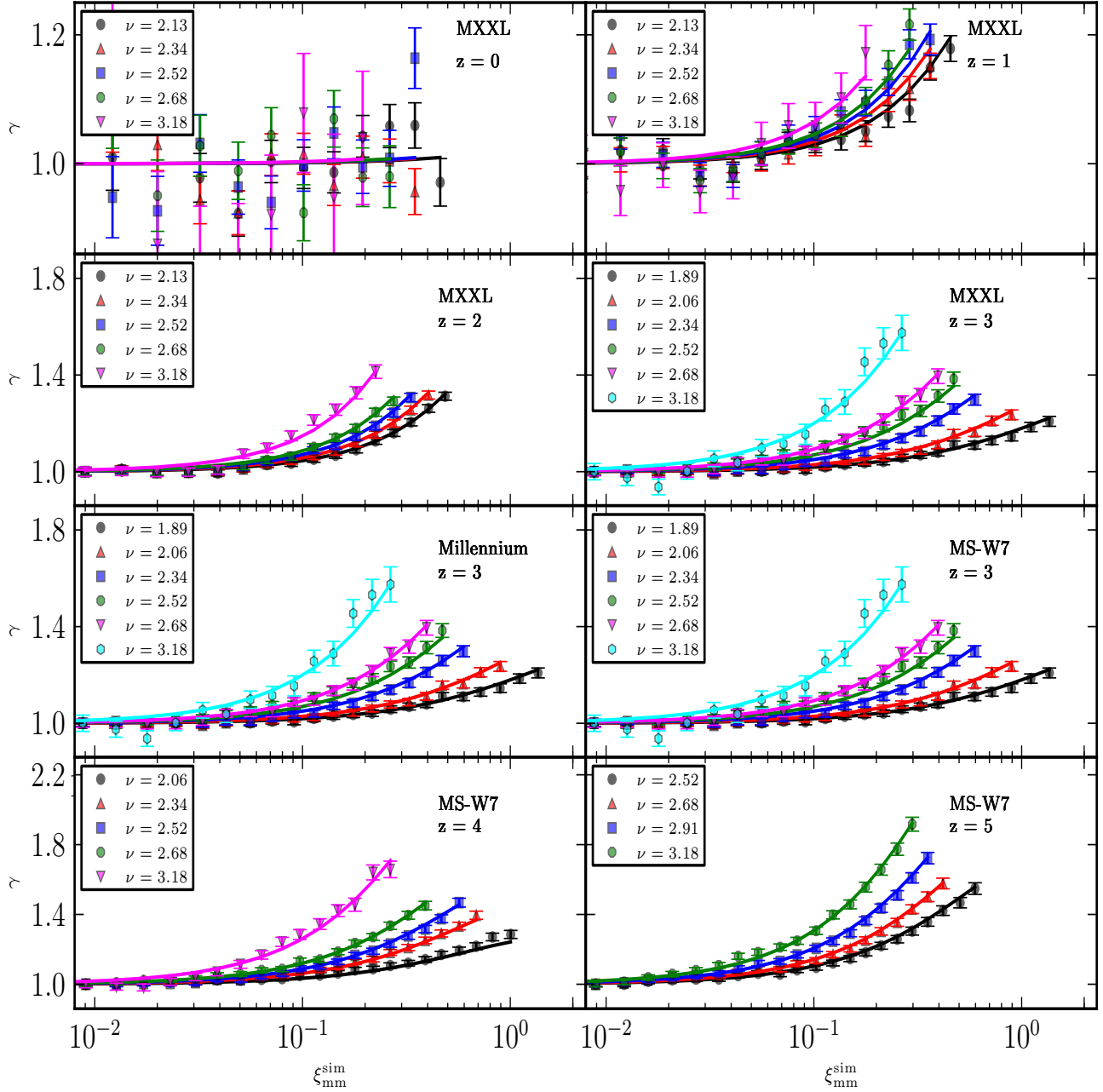


Figure 7. Our fitting function for the scale dependence of the non-linear bias, $\gamma(\xi_{\text{mm}}^{\text{sim}}, \nu, \alpha_m, \Omega_m^z)$, in the redshift range 0–5 as a function of $\xi_{\text{mm}}^{\text{sim}}(r)$ for various choices of ν (see legend) is shown using solid lines. The N-body simulation from which results were measured along with the redshift is labelled on each panel.

$z = 3, 4$ and 5 are obtained for the MS-W7 and the red circles at lower redshifts are for the MXXL cosmological parameters. The figure clearly shows that $\alpha_m(z)$ is nearly constant in the redshift range 3–5 for the MS-W7 cosmology. However, at $z = 2$ where the MXXL cosmology is used, $\alpha_m(z)$ is larger. Such a difference is perhaps related to the departure from the universal nature of non-linear bias as a function of $\nu(M, z)$ and $\xi_{\text{mm}}^{\text{sim}}(r, z)$. Motivated by this, we further investigated whether $\gamma(M, r, z)$ can be expressed as a function of $\nu(M, z)$, $\xi_{\text{mm}}^{\text{sim}}(r, z)$ and $\alpha_m(z)$ and we find that, it is indeed possible to obtain a good fit for high- σ halos ($\nu > 1$). The

resulting fitting function is given by

$$\gamma(\xi_{\text{mm}}^{\text{sim}}, \nu, \alpha_m) = \left(1 + K_0(1 + k_3\alpha_m) \log\left(1 + \xi_{\text{mm}}^{\text{sim} k_1}\right) \nu^{k_2}\right) \times \left(1 + L_0(1 + l_3\alpha_m) \log\left(1 + \xi_{\text{mm}}^{\text{sim} l_1}\right) \nu^{l_2}\right) \quad (15)$$

The free parameters are estimated to be $K_0 = -0.2929$, $k_1 = 1.2451$, $k_2 = 4.2027$, $k_3 = 0.5887$, $k_4 = 15.1297$, $L_0 = 3.9654$, $l_1 = 1.1729$, $l_2 = 1.2546$, $l_3 = 0.4725$ and $l_4 = 3.3939$. In fitting Eq. (15), we have used the non-linear bias estimated from simulations for all $\nu(M, z)$ bins in redshift range $z = 2 - 5$ given in Table 1. For fitting $\gamma(\xi_{\text{mm}}^{\text{sim}}, \nu, \alpha_m)$, we con-

sidered halo correlation functions only on scales larger than twice the virial radius of the most massive halo in the sample. Moreover, we have restricted our analysis to $r \lesssim 30 h^{-1}$ Mpc.

It is also important to note from Table 1 that the masses of the halos used in our analysis range typically from 5×10^{10} to $5 \times 10^{13} h^{-1} M_\odot$. Thus, the high- σ halos of interest are those expected to host galaxies in the redshift range 2 – 5.

The expression for $\gamma(\xi_{\text{mm}}^{\text{sim}}, \nu)$ in Eq. (15) is plotted (solid line) in Fig. 6 at different redshifts as a function of $\xi_{\text{mm}}^{\text{sim}}(r)$ at that redshift and for different values of $\nu(M)$. In Fig. 6, the results shown at $z = 2$ are from the MXXL simulation and those at other redshifts are from the MS-W7 simulation. From Fig. 6, it is clear that the parameterization of $\gamma(\xi_{\text{mm}}^{\text{sim}}, \nu, \sigma_{\text{eff}})$ using Eq. (15) fits the whole range of data measured directly from the simulations very well. In particular, we note that our fit is consistent with the results from simulations to within an overall accuracy of 4%. This suggests that, it is indeed possible to find a fitting function for the scale dependence of the non-linear bias in the redshift range 2 – 5, through $\xi_{\text{mm}}^{\text{sim}}$, ν and α_m .

In Fig. 6, we have also plotted in dotted lines, the fitting function for γ given by Reed et al. (2009). These authors parameterized the scale dependence as a function of the large scale bias $b(\nu)$ and $\sigma(r, z)$ as

$$\gamma(b(\nu), \sigma(r, z)) = [1 + 0.03b^3(\nu)\sigma^2(r, z)]. \quad (16)$$

It is clear from Fig. 6 that the Reed et al. (2009) fit compares reasonably well with results from the MXXL and MS-W7 simulations at $z = 3, 4$ and 5, especially at $z = 5$. However, their formula is not quite consistent with the MXXL simulation results at $z = 2$. This is expected, since the Reed et al. (2009) expression for non-linear bias of a halo of mass M at a scale r depends only on the dark matter power spectrum through the *rms* linear density fluctuations on the mass scale M and length scale r . As noted before, such a simple dependence cannot accurately account for the scale dependence of the non-linear bias seen from simulations.

3.5 The evolution of $\gamma(M, r, z)$ to low redshifts

Having obtained a fitting function for $\gamma(r, M, z)$ for high- z halos in the entire redshift range 2 – 5, we now include low- z data to probe the evolution of the scale-dependence of non-linear bias from $z = 0$ to 5. We note from Table 1 that, at $z = 0$ and 1, the masses of the rare dark matter halos used in our study ranges from 10^{12} to $10^{15} h^{-1} M_\odot$; correspondingly they host galaxies as well as groups and clusters.

In Fig. 7, we show $\gamma(r, M, z)$ estimated from the simulations (symbols) over the full redshift range. The data at $z = 3, 4$ and 5 are measured from MS-W7 and those at $z = 0, 1$ and 2 are from the MXXL simulation. It is clear from the figure that at lower redshifts ($z = 0$ and 1) the scale dependence of the non-linear bias is rather weaker compared to other redshifts. In particular, at $z = 0$, the halo bias increases by only $\sim 10\%$ on quasi-linear scales even for the most massive and hence rarest halos at that redshift.

It turns out that one can obtain a fit for the non-linear bias which extends to redshift 0 by adding an additional parameter, $\Omega_m(z)$, the matter density of the universe at a

given redshift.

$$\Omega_m(z) = \frac{\Omega_m(1+z)^3}{\Omega_m(1+z)^3 + \Omega_\Lambda}. \quad (17)$$

Thus, the evolution of $\gamma(r, M, z)$ in the redshift range 0 – 5 can be expressed as a function of four variables, $\Omega_m(z)$, $\nu(M, z)$, $\xi_{\text{mm}}^{\text{sim}}(r, z)$ and $\alpha_m(z)$. In particular, we obtained a fitting function for $\gamma(r, M, z)$ using the non-linear bias estimated from simulations for halos in bins of $\nu(M, z)$ in the redshift range $z = 0 - 5$ given in Table 1. As before, we have used the correlation functions only on scales larger than twice the virial radius of the biggest halo in the sample and smaller than 30 Mpc/h for the analysis. The resulting fitting function is given by,

$$\begin{aligned} \gamma(\xi_{\text{mm}}^{\text{sim}}, \nu, \alpha_m, \Omega_m(z)) = & \\ & \left(1 + K_0(1 + k_3\alpha_m)(\Omega_m(z))^{k_4} \log\left(1 + \xi_{\text{mm}}^{\text{sim} k_1}\right) \nu^{k_2}\right) \times \\ & \left(1 + L_0(1 + l_3\alpha_m)(\Omega_m(z))^{l_4} \log\left(1 + \xi_{\text{mm}}^{\text{sim} l_1}\right) \nu^{l_2}\right) \end{aligned} \quad (18)$$

Here $K_0 = 0.1699$, $k_1 = 1.194$, $k_2 = 4.311$, $k_3 = 0.1536$, $k_4 = 17.8283$, $L_0 = 2.9138$, $l_1 = 1.3502$, $l_2 = 1.9733$, $l_3 = 0.4537$ and $l_4 = 3.1731$. The fitting function in Eq. (18) is plotted as solid lines in Fig. 7 along with data points measured from simulations. Our fit is in remarkable agreement with data from all the simulations over the entire range of redshifts from 0 to 5, peak heights and length scales. The overall agreement of this fit with the data from the simulations is found to be better than 4%.

3.6 Halo clustering as a function of the linear matter correlation function

We have, so far, presented an analytical model for the non-linear clustering of dark matter halos as a function of the non-linear dark matter correlation function, $\xi_{\text{mm}}^{\text{sim}}(r, z)$, measured from the simulations. In this section, we model halo clustering as a function of the linear matter correlation function, $\xi_{\text{mm}}^{\text{lin}}(r, z)$. This is well motivated because $\xi_{\text{mm}}^{\text{lin}}(r, z)$ is easier to compute without uncertainties, compared to the non-linear matter correlation function. Thus, for all practical purposes, it will be convenient to express the non-linear bias as a function of $\xi_{\text{mm}}^{\text{lin}}(r, z)$. The linear matter correlation function is computed from the linear matter power spectrum $P^{\text{lin}}(k, z)$ as

$$\xi_{\text{mm}}^{\text{lin}}(r, z) = \int_0^\infty \frac{dk}{2\pi^2} k^2 P^{\text{lin}}(k, z) \frac{\sin(kr)}{kr}. \quad (19)$$

In order to model the non-linear halo bias as a function of $\xi_{\text{mm}}^{\text{lin}}(r, z)$, we first define $b_{\text{nl}}(r, M, z)$ at any given scale as

$$b_{\text{nl}}(r, M, z) = \sqrt{\frac{\xi_{\text{hh}}^{\text{sim}}(r, z)}{\xi_{\text{mm}}^{\text{lin}}(r, z)}}. \quad (20)$$

The new definition of $b_{\text{nl}}(r, M, z)$ is similar to that given by Eq. (10), but uses $\xi_{\text{mm}}^{\text{lin}}(r, z)$ instead of $\xi_{\text{mm}}^{\text{sim}}(r, z)$. Following section 3.2 we then express the non-linear bias as the product of the scale-independent large scale bias $b(\nu)$ and the scale-dependent function $\gamma(r, M, z)$ (see Eq. (11)). A new fitting function is obtained for the large scale bias by re-fitting the free parameters of Eq. (4) to the large scale bias

measured from the simulations. The new best fit parameters are given by $A = 1.0$, $a = 0.223$, $B = 1.156$, $b = 2.167$, $C = -0.748$ and $c = 2.167$.

As before, we find that, the scale-dependence of halo bias $\gamma(r, M, z)$ can be expressed as a function of ν , α_m , $\Omega_m(z)$ and the linear matter correlation function, $\xi_{\text{mm}}^{\text{lin}}$. The fitting function for γ is assumed to have the same functional form as in Eq. (18) with $\xi_{\text{mm}}^{\text{sim}}$ being replaced by $\xi_{\text{mm}}^{\text{lin}}$. The free parameters of Eq. (18) are then determined by fitting this equation to the data measured from all the simulations in the redshift range 0 – 5. The new best fit parameters of Eq. (18) are given by $K_0 = 0.000529$, $k_1 = 1.0686$, $k_2 = 3.4158$, $k_3 = -204.1715$, $k_4 = 26.9453$, $L_0 = 0.448$, $l_1 = 2.128$, $l_2 = 3.0222$, $l_3 = 0.226$ and $l_4 = 1.691$. We emphasize that the new fit for γ as function of $\xi_{\text{mm}}^{\text{lin}}$ agrees very well with the simulation data. The overall agreement of this fit with the data from all the simulations given in Table 1 is found to be better than 5%.

4 DISCUSSION AND CONCLUSIONS

We have revisited the problem of modelling the non-linear clustering of rare dark matter halos, that collapse from 1–3 σ fluctuations, on quasi-linear scales. In particular, we found using high-resolution N-body simulations that the non-linear bias of high redshift galactic dark matter halos is strongly scale dependent on scales $\sim 0.5 - 10 h^{-1}$ Mpc. These scales, commonly referred to as quasi-linear scales, correspond to scales larger than the typical virial radii of dark matter halos. Even though we primarily focussed on the clustering of dark matter halos in the redshift range 0 – 5, our results are applicable to higher redshifts, including the cosmic dark ages before the epoch of reionization.

First, we estimated the correlation functions of dark matter halos at $z = 2, 3, 4$ and 5 from the N-body simulations, in mass bins in the mass range $10^{11} - 4 \times 10^{12} M_\odot$. These are the typical masses of dark matter halos that host LBGs and LAEs in the same redshift range and correspond to rarer objects collapsing from high σ fluctuations (Jose et al. 2013b). We then showed that, on quasi-linear scales, there is a strong discrepancy between the halo correlation functions computed using the scale independent, linear halo bias and those measured directly from simulations. This suggests that the linear bias approximation is not sufficient to explain the clustering of high- z , rarer dark matter halos on quasi-linear scales.

To quantify the non-linear bias of dark matter halos in this redshift range, we measured the correlation functions of halos, from simulations, in bins of halo peak height, $\nu(M, z)$. The non-linear bias is defined as the square root of the ratio of halo and dark matter correlation functions (see Eq. (10)). We found that the non-linear bias of a halo can be expressed as the product of the usual scale independent large scale bias $b(M, z)$ and a scale dependent function $\gamma(r, M, z)$ (Eq. (11)). We also obtained a fitting function for $b(M, z)$ which depends only on the peak height, $\nu(M, z)$, of dark matter halos. This fit compares very well with other formulae for large scale bias in the literature (Sheth & Tormen 1999; Tinker et al. 2010), especially for halos with $\nu \lesssim 2$, collapsing from low σ fluctuations. For rarer halos with larger values of ν , we obtained a slightly lower value for the large scale bias com-

pared to the formula given by Tinker et al. (2010). However, as noted before, this could be due to the difference between the SO and FOF(0.2) halo finder algorithms respectively used by Tinker et al. (2010) and in our work. Further, both studies use distinct simulations with different cosmological parameters for calibrating the bias.

We find that, for $z = 2 - 5$, the scale dependence of the non-linear bias, $\gamma(r, M, z)$, for halos of mass M at any length scale r depends on three parameters, the peak height, $\nu(M, z)$, of halos at mass M , the dark matter correlation function ($\xi_{\text{mm}}^{\text{sim}}(r, z)$) at that length scale and α_m , an effective power law index of $\sigma(M)$ at that redshift. We obtained a fitting function that describes the scale dependence of $\gamma(r, M, z)$ as a function of these parameters in the same redshift range. Our fit agrees with the simulation results within an accuracy of 4%.

The scale dependence of non-linear bias at a scale r is usually parametrized in real space using $\xi_{\text{mm}}^{\text{sim}}(r, z)$ (Tinker et al. 2005) or the *rms* linear overdensity in uniformly overdense spheres of radius r , $\sigma(r, z)$ (Hamana et al. 2001; Diaferio et al. 2003; Reed et al. 2009). Both $\sigma(r, z)$ and $\xi_{\text{mm}}^{\text{sim}}(r, z)$ can be expressed as functions of the dark matter power spectrum. However, we find that the scale dependence of the bias, as quantified in terms of $\gamma(r, M, z)$, is not described by such parametrizations, but rather depends on the quantity $\alpha_m(z)$. But, to compute $\alpha_m(z)$, one requires only the linear dark matter power spectrum. Therefore, it can be argued that at high redshifts ($z \geq 2$) the non-linear bias is a universal function of the dark matter power spectrum.

We extended our analysis by probing the non-linear bias of low redshift, rarer dark matter halos on quasi-linear scales, using MXXL halos at $z = 0$ and 1. Interestingly at lower redshifts, especially at $z \sim 0$, the scale dependence of non-linear bias is weaker than at high redshifts and is within 10-20 % of the large scale bias measured from simulations at any scale. We propose a fitting function for the non-linear bias as a function of the matter density of the universe at a given redshift ($\Omega_m(z)$) along with $\nu(M, z)$, $\xi_{\text{mm}}^{\text{sim}}(r, z)$ and $\alpha_m(z)$. Remarkably, this fitting function, calibrated using the MS-W7 and MXXL simulations, captures the redshift evolution of non-linear bias for a wide range of halo masses and length scales within an overall accuracy of 4%.

The dependence of $\gamma(r, M, z)$ on $\Omega_m(z)$ at low redshifts breaks the universality of the non-linear bias with respect to the linear matter fluctuation field. Thus the observed large scale bias of any galaxy population, which depends only on the dark matter power spectrum through $\nu(M, z)$, will not uniquely determine the scale dependence of the bias. This may provide an opportunity to use the scale-dependence of halo bias as a valuable tool to probe cosmology, particularly the matter density of the universe.

We have also extended our analysis by expressing the non-linear bias as a function of the linear matter correlation function, $\xi_{\text{mm}}^{\text{lin}}(r, z)$. Here also the non-linear bias is expressed as the product of the scale independent large scale bias, $b(M, z)$, and the scale dependent function, $\gamma(r, M, z)$. We first obtained a fitting function for the large scale bias as a function of $\nu(M, z)$. An analytical fit for $\gamma(r, M, z)$ is then obtained as a function of linear matter correlation function, $\xi_{\text{mm}}^{\text{lin}}(r, z)$, along with $\nu(M, z)$, $\alpha_m(z)$ and $\Omega_m(z)$. The new fit for γ agrees with the data from the simulations within an accuracy better than 5%. We emphasize that this model

parameterizes the clustering of dark matter halos as a function of $\xi_{\text{mm}}^{\text{lin}}(r, z)$ instead of the non-linear matter correlation function. Such a model could be quite useful for practical purposes as it is easier to compute $\xi_{\text{mm}}^{\text{lin}}(r, z)$ analytically without uncertainties compared to the non-linear matter correlation function.

In general, the halo bias of high redshift, rare dark matter halos is significantly non-linear and scale dependent on quasi-linear scales. On the other hand, at $z = 0$, this scale dependence is quite weak and seems to be dependent on the matter density of the universe. The non-linear bias is expected to have interesting implications on observations of the high redshift universe. For example, the halo occupation distribution modelling of LBG clustering at high- z ($z \geq 3$) usually assumes a linear halo bias (Hamana et al. 2004, 2006; Hildebrandt et al. 2009; Lee et al. 2009; Jose et al. 2013b). However, at these redshifts, the typical LBGs collapse from $2 - 3\sigma$ fluctuations. Hence, one has to incorporate the non-linear bias to improve the clustering predictions of LBGs on quasi-linear scales. Thus the non-linear bias could change the predicted shape of the two point correlations functions of high redshift LBGs and also LAEs, quasars and even the redshifted 21 cm signals from the pre-reionization. It would be interesting to explore the implications of the non-linear and scale-dependent bias in the high- z universe. However, we leave this for future work.

ACKNOWLEDGMENTS

CJ thanks Kandaswamy Subramanian, Raghunathan Sri-anand and Aseem Paranjpaye for useful discussions. CJ acknowledges partial support from the Institute for Computational Cosmology (ICC), Durham University while visiting the ICC and Carlos Frenk at the ICC for warm hospitality. This work was supported by the Science and Technology Facilities Council [ST/L00075X/1]. This work used the DiRAC Data Centric System at Durham University, operated by the ICC on behalf of the STFC DiRAC HPC Facility (www.dirac.ac.uk). This equipment was funded by BIS National E-infrastructure capital grant ST/K00042X/1, STFC capital grant ST/H008519/1, and STFC DiRAC Operations grant ST/K003267/1 and Durham University. DiRAC is part of the UK's National E-Infrastructure.

REFERENCES

- Angulo R. E., Baugh C. M., Frenk C. S., Bower R. G., Jenkins A., Morris S. L., 2005, *MNRAS*, 362, L25
- Angulo R. E., Baugh C. M., Lacey C. G., 2008, *MNRAS*, 387, 921
- Angulo R. E., Springel V., White S. D. M., Jenkins A., Baugh C. M., Frenk C. S., 2012, *MNRAS*, 426, 2046
- Bardeen J. M., Bond J. R., Kaiser N., Szalay A. S., 1986, *ApJ*, 304, 15
- Bond J. R., Cole S., Efstathiou G., Kaiser N., 1991, *ApJ*, 379, 440
- Boylan-Kolchin M., Springel V., White S. D. M., Jenkins A., Lemson G., 2009, *MNRAS*, 398, 1150
- Cen R., Dong F., Bode P., Ostriker J. P., 2004, *ArXiv Astrophysics e-prints*
- Cole S. et al., 2005, *Monthly Notices of the Royal Astronomical Society*, 362, 505
- Cooray A., Sheth R., 2002, *Phys. Rep.*, 372, 1
- Davis M., Efstathiou G., Frenk C. S., White S. D. M., 1985, *ApJ*, 292, 371
- Desjacques V., Crocce M., Scoccimarro R., Sheth R. K., 2010, *Phys. Rev. D*, 82, 103529
- Diaferio A., Nusser A., Yoshida N., Sunyaev R. A., 2003, *MNRAS*, 338, 433
- Fry J. N., Gaztanaga E., 1993, *ApJ*, 413, 447
- Gao L., White S. D. M., Jenkins A., Frenk C. S., Springel V., 2005, *MNRAS*, 363, 379
- Guo Q., White S., Angulo R. E., Henriques B., Lemson G., Boylan-Kolchin M., Thomas P., Short C., 2013, *MNRAS*, 428, 1351
- Hamana T., Ouchi M., Shimasaku K., Kayo I., Suto Y., 2004, *MNRAS*, 347, 813
- Hamana T., Yamada T., Ouchi M., Iwata I., Kodama T., 2006, *MNRAS*, 369, 1929
- Hamana T., Yoshida N., Suto Y., Evrard A. E., 2001, *ApJ*, 561, L143
- Hildebrandt H., Pielorz J., Erben T., van Waerbeke L., Simon P., Capak P., 2009, *A&A*, 498, 725
- Huff E., Schulz A., White M., Schlegel D., Warren M., 2007, *Astroparticle Physics*, 26, 351
- Iliev I. T., Scannapieco E., Martel H., Shapiro P. R., 2003, *MNRAS*, 341, 81
- Jenkins A., Frenk C. S., White S. D. M., Colberg J. M., Cole S., Evrard A. E., Couchman H. M. P., Yoshida N., 2001, *MNRAS*, 321, 372
- Jose C., Srianand R., Subramanian K., 2013a, *MNRAS*, 435, 368
- Jose C., Subramanian K., Srianand R., Samui S., 2013b, *MNRAS*, 429, 2333
- Kaiser N., 1984, *ApJ*, 284, L9
- Larson D. et al., 2011, *ApJS*, 192, 16
- Lee K.-S., Gialavalis M., Conroy C., Wechsler R. H., Ferguson H. C., Somerville R. S., Dickinson M. E., Urry C. M., 2009, *ApJ*, 695, 368
- Matsubara T., 1999, *The Astrophysical Journal*, 525, 543
- Mo H. J., White S. D. M., 1996, *MNRAS*, 282, 347
- Musso M., Paranjape A., Sheth R. K., 2013, *Monthly Notices of the Royal Astronomical Society*, 427, 3145
- Paranjape A., Sefusatti E., Chan K. C., Desjacques V., Monaco P., Sheth R. K., 2013, *MNRAS*, 436, 449
- Peebles P. J. E., 1980, *The large-scale structure of the universe*. Princeton University Press, Princeton, N.J.
- Pike S. R., Kay S. T., Newton R. D. A., Thomas P. A., Jenkins A., 2014, *MNRAS*, 445, 1774
- Reed D. S., Bower R., Frenk C. S., Jenkins A., Theuns T., 2009, *MNRAS*, 394, 624
- Scannapieco E., Barkana R., 2002, *ApJ*, 571, 585
- Scannapieco E., Thacker R. J., 2005, *ApJ*, 619, 1
- Seo H., Eisenstein D. J., 2005, *The Astrophysical Journal*, 633, 575
- Sheth R. K., Mo H. J., Tormen G., 2001, *MNRAS*, 323, 1
- Sheth R. K., Tormen G., 1999, *MNRAS*, 308, 119
- Smith R., Scoccimarro R., Sheth R., 2007, *Physical Review D*, 75, 063512
- Smith R. E. et al., 2003, *MNRAS*, 341, 1311
- Springel V. et al., 2005, *Nature*, 435, 629
- Tinker J., Kravtsov A. V., Klypin A., Abazajian K., War-

ren M., Yepes G., Gottlöber S., Holz D. E., 2008, ApJ, 688, 709

Tinker J. L., Robertson B. E., Kravtsov A. V., Klypin A., Warren M. S., Yepes G., Gottlöber S., 2010, ApJ, 724, 878

Tinker J. L., Weinberg D. H., Zheng Z., Zehavi I., 2005, ApJ, 631, 41

APPENDIX A: THE EFFECTIVE POWER LAW INDEX OF $\sigma(M)$

For any mass scale M , the variance of smoothed density contrast $\sigma^2(M) \propto k_M^3 P(k_M) \sigma_8^2 k_M^{3+n_{\text{eff}}}$ (Peebles 1980). Here n_{eff} is the effective spectral index, which is ~ -2 on galactic scales and -1 on cluster scales. We also have $k_M^{-1} \sim M^{1/3}$. Thus we get

$$\sigma(M) \propto M^{\frac{-(3+n_{\text{eff}})}{6}} \propto M^{-\alpha}. \quad (\text{A1})$$

Given the non-linear mass, M_{nl} , and collapse mass, M_{col} , corresponds to the mass scales where $\sigma(M)$ is respectively 1 and 1.686, it is possible to define an effective power law index α_m as

$$\frac{\sigma(M_{col})}{\sigma(M_{nl})} = 1.686 = \left(\frac{M_{col}}{M_{nl}} \right)^{-\alpha_m} \quad (\text{A2})$$

Thus we have

$$\alpha_m = \frac{\log(1.686)}{\log(M_{nl}/M_{col})} = 0.2269 \left[\log \frac{M_{nl}}{M_{col}} \right]^{-1} \quad (\text{A3})$$